

## Cone-Beam Reconstruction of Plate-Like Specimens

G. WANG, T.H. LIN, P.C. CHENG, D.M. SHINOZAKI

Advanced Microscopy and Imaging Laboratory (AMIL) and Advanced Real Time System Laboratory (ARTS), Department of Electrical and Computer Engineering, State University of New York, Buffalo, New York, USA; \* Department of Materials Engineering, Faculty of Engineering Science, University of Western Ontario, London, Ontario, Canada

**Summary:** An x-ray shadow projection microscope using a scannable point source of x-rays is under development at AMIL-ARTS, SUNY at Buffalo. Considering the characteristics of the x-ray microscope of AMIL-ARTS and the limitations of Feldkamp's cone-beam reconstruction algorithm, a general cone-beam image reconstruction algorithm has been developed. In x-ray microscopy, many specimens are plate-like. The reconstruction of a plate-like specimen appears to be a limited angle problem. A novel method is presented to reconstruct a plate-like specimen using the general cone-beam reconstruction algorithm. Shepp and Logan's head phantom is used in validating this method. A method for synthesizing projection data of ellipsoids is described. Typical simulation results are given.

### Introduction

An x-ray projection microscope using a scannable point source of x-rays is under development at AMIL-ARTS, SUNY at Buffalo (Cheng and Jan 1987, Cheng *et al.* 1989, 1990, 1991 a,b, Schmahl and Cheng 1991, Wang *et al.* 1991a). The point source is generated by a focussed electron beam, which can be steered electromagnetically in a

plane perpendicular to the optical axis of the microscope. A specimen is mounted on a rotatable and shiftable mechanical stage for microtomography. An elaborate feedback system is being implemented to measure and correct the motion error of the mechanical stage dynamically.

The cone-beam reconstruction of the x-ray images has been studied for more than 30 years. More recent reviews have been written by Smith (1990) and Gullberg *et al.* (1992). Existing cone-beam algorithms can be categorized into two broad classes: analytic and algebraic (Kak and Slaney 1987, Lewitt 1983). Algebraic algorithms demand more computing resources than analytic ones. Because a high reconstruction speed is very important, analytic algorithms are always preferred in practice. Feldkamp *et al.* (1984) proposed an extension of the equispacial fan-beam reconstruction algorithm (Kak and Slaney 1987), where two-dimensional projection data from different angles are filtered and back-projected to voxels along projection beams. The reconstructed value of a voxel is the sum of contributions from all tilted fan-beams passing through the voxel. Considering the characteristics of the x-ray microscope system of AMIL-ARTS and the limitations of Feldkamp's cone-beam reconstruction algorithm, a general cone-beam image reconstruction algorithm has been developed at AMIL-ARTS (Wang *et al.* 1991 b, 1992 a, b). The general cone-beam algorithm allows various scanning loci and provides the same computational efficiency and parallelism as Feldkamp's algorithm.

In the next section, the general cone-beam reconstruction algorithm is briefly summarized. In the third section, a novel method for reconstructing a plate-like specimen is presented. In the fourth section, an algorithm for synthesizing projection data of ellipsoids is described. Finally, in the fifth section, our method is validated via simulation using Shepp and Logan's phantom.

### Reconstruction Formula

Assume that there is a scanning locus turn of the x-ray source associated with each horizontal slice of a specimen. Such a locus turn can be defined in cylindrical coordinates by the following equation:

$$\rho = \rho(\beta), h = h(\beta), \beta \in [0, 2\pi]. \quad (1)$$

---

This work was supported by grants from the U.S. National Institute of Health—Biomedical Research Grant Program (BRSG S07 RR07066,) the U.S. National Science Foundation (NSF MIP-9010948), the U.S. Dept. of Energy (DE-AS08-88DP 10782, DE-FG03-89SF18012), Whitaker Foundation (Program for Biomedical Engineering); and by NSERC (Canada) (Operating and Strategic Grants), the Ontario Center for Materials Research, and the Canadian Synchrotron Radiation Facility (CSRF). The content of this paper was presented at Int. Simulation Tech Conference, Orlando, Florida, October 1991.

Address for reprints:

Ge Wang  
Department of Electrical and Computer Engineering  
State University of New York  
Buffalo, NY 14260, USA

The projection data collected from a locus turn are used to reconstruct the corresponding slice, which is also referred to as the mid-plane. In a three-dimensional coordinate system  $(x, y, z)$ , the cone-beam reconstruction is performed by tilting the fan out of the mid-plane, thus changing the coordinate system  $(t, s)$  which denotes the rotated coordinate system described by

$$t = x \cos \beta + y \sin \beta, \quad s = -x \sin \beta + y \cos \beta, \quad (2)$$

where  $\beta$  is the rotation angle of the specimen. A new coordinate system  $(\tilde{t}, \tilde{s})$  is defined to represent the location of a reconstructed point with respect to the tilted fan. Considering the geometry of the tilted fan, both the source-to-origin distance and the angular differential are modified. After the modification, it follows that

$$g(x, y, z) = \frac{1}{2} \int_0^{2\pi} \frac{\rho^2(\beta)}{(\rho(\beta) - s)^2} \int_{-\infty}^{\infty} R_{\beta}(p, \zeta) f\left(\frac{\rho(\beta)t}{\rho(\beta) - s} - p\right) \frac{\rho(\beta)}{\sqrt{\rho^2(\beta) + p^2 + \zeta^2}} dp d\beta, \quad (3)$$

where  $R_{\beta}(p, \zeta)$  is the two-dimensional equispacial cone-beam projection data,  $f(\cdot)$  is the reconstruction filter,

$$\zeta = \frac{\rho(\beta)\tilde{z}(\beta)}{\rho(\beta) - s},$$

and the local coordinate system  $[x, y, \tilde{z}(\beta)]$  associated with angle  $\beta$  is defined by:

$$\tilde{z}(\beta) = z - h(\beta).$$

Equation (3) is called the general cone-beam reconstruction formula. (Wang *et al.* 1991b, 1992 a, b).

## Method

In practical cases of microscopy, many specimens are rather plate-shaped, as in typical thick film sections. The reconstruction of a plate-like sample appears to be a limited-angle problem which can be addressed using standard methods described previously in the literature. Since the methods based on a point source and projection microscopy have great advantages experimentally, a novel scheme is developed to reconstruct plate-like specimens using the general cone-beam algorithm (Wang *et al.* 1991c). The method is explained as follows (Fig. 1).

Assume that the locus of the x-ray source is a two-dimensional curve (e.g., it may be a circle, polygon, or a rectangle). The plate-like specimen (or thick film) is placed parallel to the plane of the source locus. Arrange the relative position so that the perpendicular passing through the center of the scanning locus passes through the center of the specimen area of interest. This perpendicular is labeled

the principal axis. The specific locus used is made to be similar to the shape of the area of interest and substantially larger than that area. The detector plane is placed behind the specimen, parallel to the specimen, and the two-dimensional projection data recorded for each x-ray source position. After each frame of these projection data is mapped onto the plane facing the x-ray source and passing through the principal axis, the general cone-beam algorithm is applied to the modified projection data. In this way the problems associated with the standard limited angle approaches are avoided.

## Projection Data Synthesis

A three-dimensional version of the Shepp and Logan's head phantom was used as the specimen. To obtain the three-dimensional head phantom, the two-dimensional ellipses of the conventional head phantom have been made into ellipsoids (Kak and Slaney 1987). This phantom is typical as it contains sharp density changes, thin surfaces, small objects, asymmetrical structures, and so on. Projection data are formed from the phantom as analytically derived line integrals of the x-ray absorption coefficient from the x-ray source to each detector position.

A ray of a three-dimensional projection is described by the intersection of two planes

$$t = x \cos \theta + y \sin \theta, \quad (4)$$

$$r = (-x \sin \theta + y \cos \theta) \sin \gamma + z \cos \gamma. \quad (5)$$

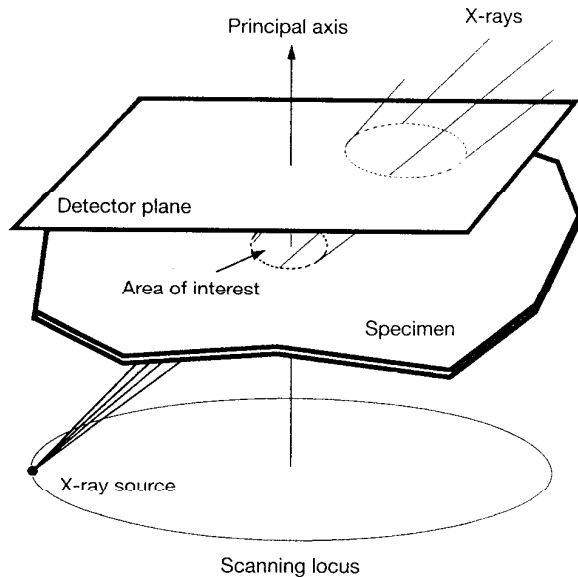


FIG. 1 Schematic diagram illustrating the arrangement for cone-beam reconstruction of a plate-like specimen.

A new coordinate system  $(t,s,r)$  is obtained by two rotations of the  $x,y,z$  axes. The first rotation, as in the two-dimensional case, is by  $\theta$  degrees around the  $z$  axis to give the  $t,s',z$  axes. The  $\theta$  angle is measured counter-clockwise (i.e., from  $x$  axis to  $t$  axis). Then the second rotation is done out of the  $t-s'$  plane around the  $t$  axis by an angle of  $\gamma$ . The  $\gamma$  angle is measured clockwise, in other words, from  $z$  axis to  $r$  axis. In matrix form the required rotations are described by

$$\mathbf{x} = \begin{pmatrix} \cos \theta & -\sin \theta \cos \gamma & -\sin \theta \sin \gamma \\ \sin \theta & \cos \theta \cos \gamma & \cos \theta \sin \gamma \\ 0 & -\sin \gamma & \cos \gamma \end{pmatrix} \mathbf{x}' \quad (6)$$

where  $\mathbf{x} = (x,y,z)^t$  and  $\mathbf{x}' = (t,s,r)^t$ .

A three-dimensional parallel projection of the object  $i(t,s,r)$  along the ray described by (5) is then expressed by the following integral

$$P_{\theta,\gamma}(t,r) = \int_{-\infty}^{\infty} i(t,s,r) ds \quad (7)$$

Note that four variables are being used to specify the desired ray;  $(t,\theta)$  specify the distance and angle in the  $x$ - $y$  plane and  $(r,\gamma)$  in the  $s$ - $z$  plane.

In a cone-beam system, assume the source is rotated by  $\beta = 0$  and ray integrals measured on the detector plane are described by  $R_{\beta=0}(p',\zeta')$ , where  $p',\zeta'$  represent horizontal and vertical axes, respectively, in the coordinate system of the detector plane. To find the equivalent parallel projection ray, first define that

$$p = \frac{p' \rho}{\rho + \rho_d} \text{ and } \zeta = \frac{\zeta' \rho}{\rho + \rho_d} \quad (8)$$

to make the detector plane  $p'-\zeta'$  pass through the origin of our reconstruction coordinate system and become the  $p$ - $\zeta$  plane, where the center of rotation is the origin of the reconstruction coordinate system,  $\rho$  denotes the distance from the origin to the source, and  $\rho_d$  the distance from the origin to the detector. For a given cone-beam ray corresponding to  $R_{\beta=0}(p,\zeta)$ , the parallel projection ray is given as follows.

$$t = \rho \sin \theta, \quad (9)$$

$$\theta = \begin{cases} \arctan(\frac{p}{\rho}), & \text{if } \frac{p}{\rho} \geq 0; \\ \pi + \arctan(\frac{p}{\rho}), & \text{otherwise.} \end{cases} \quad (10)$$

$t$  and  $\theta$  locate a ray in a given tilted fan. And,

$$r = \rho |\cos \theta \sin \gamma|, \quad (11)$$

$$\gamma = \begin{cases} \gamma', & \text{if } p \geq 0 \text{ and } \zeta \geq 0; \\ \pi - \gamma', & \text{if } p \geq 0 \text{ and } \zeta < 0; \\ 2\pi - \gamma', & \text{if } p < 0 \text{ and } \zeta \geq 0; \\ \pi + \gamma', & \text{if } p < 0 \text{ and } \zeta < 0, \end{cases} \quad (12)$$

where

$$\gamma' = \left| \arctan \left( \frac{\zeta}{\sqrt{\rho^2 + p^2}} \right) \right|$$

$r$  and  $\gamma$  specify the location of the tilted fan itself.

Because of the linearity of the Radon transform, a projection of an object consisting of ellipsoids is simply the sum of the projection values of all ellipsoids. If the absorption coefficient of an ellipsoid is constant and described by

$$i(x,y,z) = \begin{cases} \rho, & \frac{x^2}{A^2} + \frac{y^2}{B^2} + \frac{z^2}{C^2} \leq 1; \\ 0, & \text{otherwise,} \end{cases} \quad (13)$$

then its projection on the detector plane can be derived as follows. Using (6), the ellipsoid can then be described by the following equation:

$$\frac{(t \cos \theta - s \sin \theta \cos \gamma - r \sin \theta \sin \gamma)^2}{A^2} + \frac{(t \sin \theta + s \cos \theta \cos \gamma + r \cos \theta \sin \gamma)^2}{B^2} + \frac{(-s \sin \gamma + r \cos \gamma)^2}{C^2} = 1. \quad (14)$$

That is,

$$(a_1 s + a_0)^2 + (b_1 s + b_0)^2 + (c_1 s + c_0)^2 = 1, \quad (15)$$

where

$$\begin{aligned} a_1 &= \frac{-\sin \theta \cos \gamma}{A}, \\ a_0 &= \frac{t \cos \theta - r \sin \theta \sin \gamma}{A}, \\ b_1 &= \frac{\cos \theta \cos \gamma}{B}, \\ b_0 &= \frac{t \sin \theta + r \sin \theta \sin \gamma}{B}, \\ c_1 &= \frac{-\sin \gamma}{C}, \\ c_0 &= \frac{r \cos \gamma}{C}. \end{aligned}$$

Therefore, the projection value, as the difference of two roots of Eq. (14), can be directly computed.

If the center of the ellipsoid is at  $(x_0, y_0, z_0)$ , a coordinate system  $(x', y', z')$  can be obtained through shifting the original coordinate system  $(x, y, z)$  by the displacement  $(x_0, y_0, z_0)$ . That is,

$$\begin{aligned}x &= x' + x_0 \\y &= y' + y_0 \\z &= z' + z_0\end{aligned}\quad (16)$$

Combining (5) and (16), we can describe a ray in the coordinate system  $(x', y', z')$  as follows:

$$t - x_0 \cos \theta - y_0 \sin \theta = x' \cos \theta + y' \sin \theta, \quad (17)$$

$$\begin{aligned}r - (-x_0 \sin \theta + y_0 \cos \theta) \sin \gamma - z_0 \cos \gamma \\= (-x' \sin \theta + y' \cos \theta) \sin \gamma + z' \cos \gamma.\end{aligned}\quad (18)$$

Thus,  $t'$  and  $r'$  in the  $(x', y', z')$  coordinate system, as the counterparts of  $t$  and  $r$  in the  $(x, y, z)$  system, are:

$$t' = t - x_0 \cos \theta - y_0 \sin \theta, \quad (19)$$

$$r' = r - (-x_0 \sin \theta + y_0 \cos \theta) \sin \gamma - z_0 \cos \gamma. \quad (20)$$

The angles  $\theta$  and  $\gamma$  keep the same. If the ellipsoid is rotated by an angle  $\alpha$  around the  $z$  axis, and the source an angle  $\beta$ , the new angle  $\theta = \theta + \beta - \alpha$ .

## Simulation

The head phantom parameters are listed in Table I. There are ten ellipsoids in the phantom. In Table I,  $x_0, y_0, z_0$  specify the center of an ellipsoid,  $a, b, c$  are the  $x, y, z$  semi axes, respectively,  $\alpha$  is the rotation angle of an ellipsoid (about  $z$  axis), and  $\tau$  is a relative x-ray absorption parameter. The effective x-ray absorption coefficient of a point is the sum of the relative parameters of ellipsoids containing that point. Figure 2 shows two horizontal slices of Shepp and Logan's three-dimensional head phantom, which are with  $z = 0.625$  (left) and  $z = -0.25$  (right), respectively.

In the numerical simulation, the detector plane is  $2.2 \times 2.2$  with  $128 \times 128$  pixels and is so placed for the ease of computation that it is parallel to the scanning plane and just behind the specimen. Its center is on the principal axis. One hundred projection images with a  $3.6^\circ$  angular interval were used for the reconstruction. Figure 3 shows some recon-

TABLE I Parameters of Shepp and Logan's three-dimensional head phantom used in the simulation

No.	$x_0$	$y_0$	$z_0$	$a$	$b$	$c$	$\alpha$	$\tau$
1	0.00	0.000	0.000	0.6900	0.920	0.9000	0	2.00
2	0.00	0.000	0.000	0.6624	0.874	0.8800	0	-1.00
3	-0.22	0.000	-0.250	0.4100	0.160	0.2100	108	-0.50
4	0.22	0.000	-0.250	0.3100	0.110	0.2200	72	-0.50
5	0.00	0.350	-0.250	0.2100	0.250	0.5000	0	0.25
6	0.00	0.100	-0.250	0.0460	0.046	0.0460	0	0.50
7	-0.08	-0.650	-0.250	0.0460	0.023	0.0200	0	0.25
8	0.06	-0.650	-0.250	0.0460	0.023	0.0200	90	0.25
9	0.06	-0.105	0.625	0.0560	0.040	0.1000	90	0.50
10	0.000	0.100	0.625	0.0560	0.0560	0.1000	0	-0.50

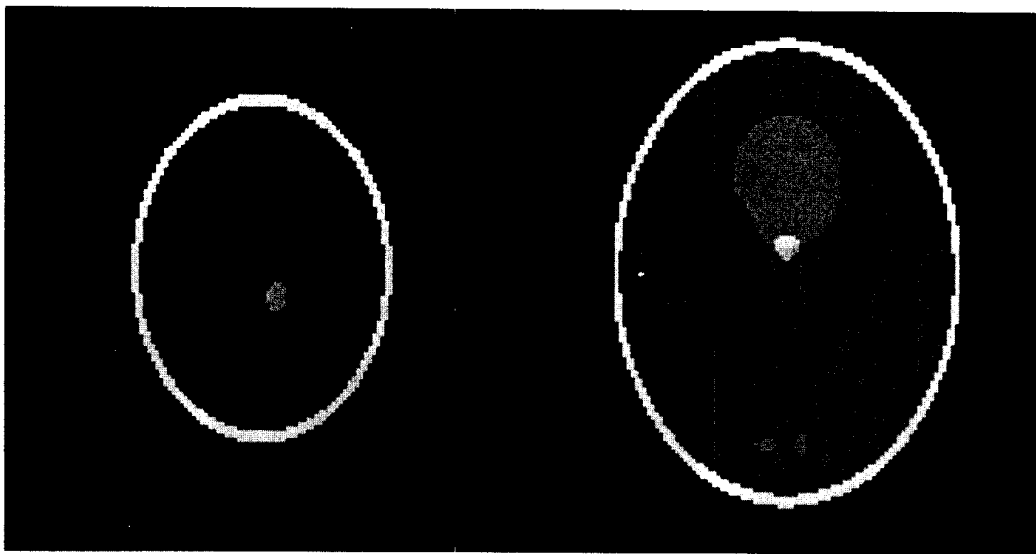


Fig. 2 Two horizontal slices of Shepp and Logan's three-dimensional head phantom at  $z = 0.625$  (left) and  $z = -0.25$  (right), respectively.

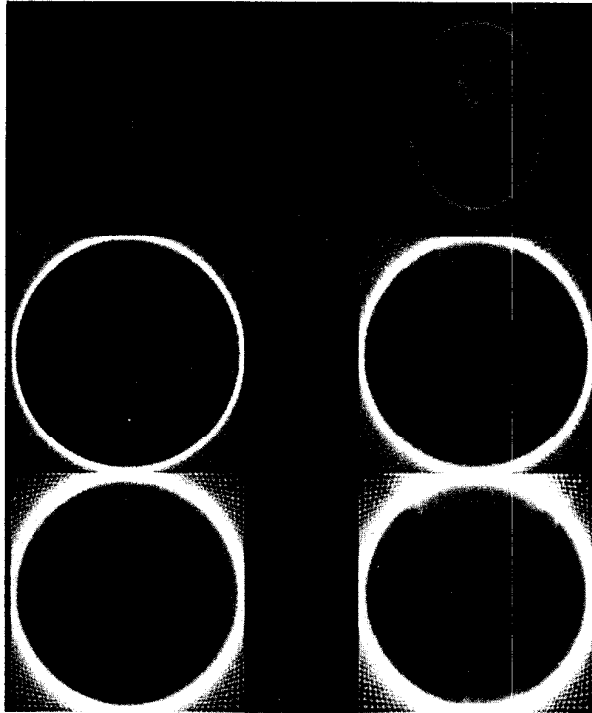


FIG. 3 Two sets of reconstructed images of a plate-like specimen for  $s = 1, 2, 5$ , respectively. The left column corresponds to the left image of Figure 1, and the right column to the right image. The scanning locus is a circle of diameter 10.

structed images of a plate-like specimen, where the scanning locus is a circle with a diameter 10, and Shepp and Logan's three-dimensional phantom was used after compressed along  $z$  axis by a factor  $k = 10$  and shifted by  $d = 0.5$ , and scaled along  $x$  and  $y$  axes by  $s = 1, 2, 5$ , respectively. Figure 3 shows that three-dimensional information of specified specimen portions is indeed obtained, even when  $s = 5$  (i.e., the plate is much larger than the reliable reconstruction region).

### Conclusion

A novel method has been developed to reconstruct plate-like specimens using the general cone-beam reconstruction algorithm. This method avoids the limited-angle

problem and gives satisfactory reconstructed images in our simulation. Therefore, our general cone-beam reconstruction algorithm can be used to reconstruct not only rod-shaped specimens (Wang 1991a) but also plate-like specimens.

### References

- Cheng PC, Jan GJ: *X-Ray Microscopy—Instrumentation and Biological Applications*. Springer-Verlag, New York (1987)
- Cheng PC, Newberry SP, Kim HG, Wittman MD: X-ray contact microradiography and shadow projection x-ray microscopy. *Eur J Cell Biol* 48 (25) 169–172 (1989)
- Cheng PC, Newberry SP, Kim HG, Wittman MD, Hwang IS: X-ray contact microradiography and shadow projection microscopy. In *Modern Microscopy* (Eds. Duke P, Michette A). Plenum Press, New York (1990) 87–117
- Cheng PC, Shinozaki DM, Lin TH, Newberry SP, Sridhar R, Targ W, Chen MT, Chen LH: X-ray shadow projection microscopy and microtomography. In *X-Ray Microscopy—III*. (Eds. Michette A, Morris GR, Buckley CJ). Springer-Verlag, Berlin (1991)
- Cheng PC, Lin TH, Shinozaki DM, Newberry SP: Projection microscopy and microtomography using x-rays. *J Scan Microsc* 13 (1), 10–11 (1991)
- Feldkamp LA, Davis LC, Kress JW: Practical cone-beam algorithm. *J Opt Soc Am* 1 (A), 612–619 (1984)
- Gullberg GT, Zeng GL, Datz FL, Christian PE, Tung CH, Morgan HT: Review of convergent beam tomography in single photon emission computed tomography. *Phys Med Biol* 37 (3), 507–534 (1992)
- Kak AC, Slaney M: *Principles of Computerized Tomographic Imaging*. IEEE Press, New York (1987)
- Lewitt RM: Reconstruction algorithms: Transform methods. *Proc IEEE* 71, 390–408 (1983)
- Schmahl G, Cheng PC: X-ray microscopy. In *Handbook on Synchrotron Radiation*, Vol. 4. (Eds. Koch TSEE, Winick H). North-Holland, Amsterdam (1991) 481–536
- Smith BD: Cone-beam tomography: Recent advances and a tutorial review. *Opt Engineering* 29, 524–534 (1990)
- Wang G, Lin TH, Cheng PC, Shinozaki DM, Newberry SP: X-ray projection microscopy and cone-beam microtomography. *Proc SPIE* 1398, 180–190 (1991a)
- Wang G, Lin TH, Cheng PC, Shinozaki DM, Kim H: Scanning cone-beam reconstruction algorithms for X-ray microtomography. *Proc SPIE*, 1556, 99–113 (1991b)
- Wang G, Lin TH, Cheng PC, Shinozaki DM: A general cone-beam reconstruction algorithm. *IEEE Trans Med Imag* (1992a) (in press)
- Wang G, Lin TH, Cheng PC, Shinozaki DM: Point spread function of the general cone-beam X-ray reconstruction formula. *Scanning* 14, 187–193 (1992b)
- Wang G, Lin TH, Cheng PC, Shinozaki DM: Simulation of cone-beam image reconstruction. *Proc SimTec '91*, (1991c) 177–182